ELSEVIER

Journal of Alloys and Compounds 323–324 (2001) 91–96

Journal of ALLOYS AND COMPOUNDS

www.elsevier.com/locate/jallcom

Crystal structure and microstructure of δ-Er_2S_3

A.R. Landa-Cánovas[a,*], U. Amador[b], L.C. Otero-Díaz[a,c]

[a]*CME Luis Bru, Univ. Complutense de Madrid, Madrid E-28040, Spain*

[b]*Dpto. Quím. Inorgánica y Materiales, Fac. CC. Experimentales y Técnicas, Univ. San Pablo, Urb. Montepríncipe, Boadilla del Monte, Madrid E-28668, Spain*

[c]*Dpto. Química Inorgánica, Fac. CC. Químicas, Univ. Complutense de Madrid, Madrid E-28040, Spain*

Abstract

The atomic structure of Er_2S_3 was refined by single-crystal X-ray diffraction methods. The compound is isostructural to the δ-Ho_2S_3 structure type, which has monoclinic symmetry and space group $P2_1/m$, $a = 10.072$ (1) Å, $b = 3.976$ (2) Å, $c = 17.389$ (2) Å, $\beta = 98.66(1)^\circ$, $Z = 6$. Refinement proceeded to $R = 0.037$ for 1745 observed reflections. Experimental high-resolution micrographs (structural images) were obtained along the [010] zone axis and compared with simulated micrographs (using the multislice Cowley–Moodie method) obtained from the average X-ray structure model. Due to electron beam damage, nanocrystallites of ErS (with NaCl-type structure) were formed on the crystal edges. Some disorder was observed by electron diffraction, probably caused by antiphase boundaries.

Keywords: Crystal growth; Crystal structure and symmetry; Scanning and transmission electron microscopy; X-ray diffraction

1. Introduction

In spite of the general similarities in the physical and chemical properties of the lanthanide elements, the crystal chemistry of their sulphides as well as their electric and magnetic properties are very complex, making it an area which has attracted the attention of many solid-state scientists [1].

It is well established that several structural types occur, polymorphism is common and there is a great variation in composition for some nominal stoichiometries. Defect structures with short-range and long-range order in the form of modulated structures also occur [2–4].

The first systematic work concerning the crystal chemistry of the rare-earth sesquisulphides was performed by Sleight and Prewit in 1968 [5]. Three structure types exist from La to Dy in the lanthanide series: A or α-Gd_2S_3 type (anti-type Cr_3C_2 [6]) is stable below 1173 K. The structure and composition of the B or β form, $Pr_{10}S_{14}O$ type, is very complex and still presents some controversy [7] and is stable between 1173 and 1473 K. Above 1473 K, the C or γ form was first described by Zachariasen as the Th_3P_4 structure type [8]. This phase is present in the range Ln_3S_4–Ln_2S_3 and has been extensively studied in the past because of its physical properties (see references cited in Ref. [1]). Very recently, Rhône-Poulenc patented the phase γ-Ce_2S_3 [9] as an ecological red pigment for plastic. Romero et al. [10] recently studied the stabilisation of γ-Ce_2S_3 by doping with carbon which goes to the cation vacant positions. The D or δ form, Ln_2S_3 for Ln = Dy to Tm, including Y, has the δ-Ho_2S_3-type structure [1], while the heaviest lanthanides, Yb and Lu, present the E or

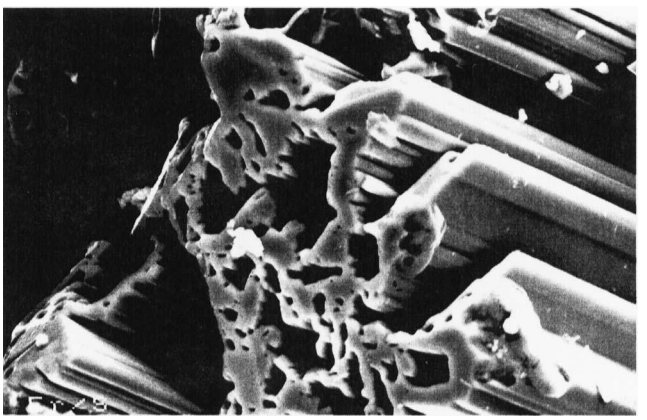

Fig. 1. Scanning micrograph of δ-Er_2S_3 needle-shaped crystals.

*Corresponding author.

E-mail address: angel@brunilda.sme.ucm.es (A.R. Landa-Cánovas).

0925-8388/01/$ – see front matter
PII: S0925-8388(01)00981-1

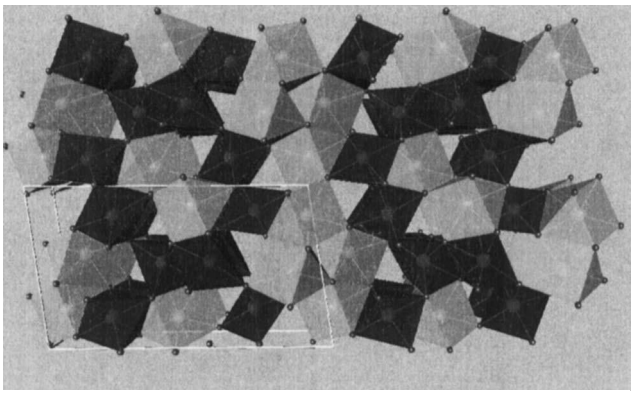

Fig. 2. Schematic drawing of the refined δ-Er_2S_3 structure where the erbium atoms are located at the centre of the polyhedra and the sulphur atoms are located at the corners of the depicted polyhedra.

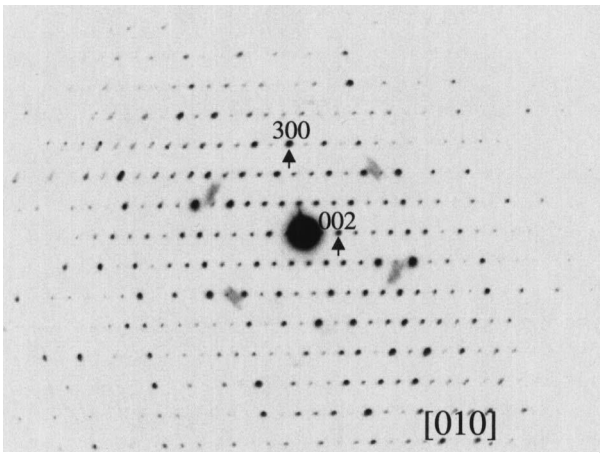

Fig. 3. SAED pattern of a δ-Er_2S_3 crystal orientated along the [010] zone axis.

Table 1
Crystal and refinement data for δ-Er_2S_3

Formula	Er_6S_9
Mol. wt.	1292.1
Crystal system	Monoclinic
Space group	$P2_1/m$
Cell dimensions (Å)	
a	10.072(1)
b	3.976(2)
c	17.389(2)
α	90.00
β	98.66(1)
γ	90.00
Z	2
V (Å^3)	688.4(4)
D_{calc} (g cm^{-3})	6.23
$F(000)$	1104
Temp. (K)	295
Diffractometer	Enraf-Nonius
Radiation	Graphited-monochromated Mo Kα ($\lambda = 0.71069$ Å)
μ(Mo Kα) (cm^{-1})	379.4
Crystal dimensions (mm)	0.1×0.1×1
2θ range (deg)	2–60
Scan technique	$\omega/2\theta$
Data collected	(−14,0,0) to (14,5,24)
Unique data	2272
Observed reflections, $I_\alpha > 3\sigma(I_0)$	1745
R_{int} (%)	2.5
Decay	–
Standard reflections	3/35
Weighting scheme	unit
$R = \Sigma\|\Delta^2 F\|/\Sigma\|F_0\|$	3.1
$R_w = (\Sigma w\Delta^2/\Sigma w\|F_0\|^2)^{1/2}$	3.7
Maximum shift/error	0.09
Absorption correction range	0.71–1.21

Table 2
Atomic parameters of Er_2S_3

Atom	X/A	Y/B	Z/C	UEQ
Er1	0.81300(7)	0.25000(0)	0.27960(5)	7(1)
Er2	0.17050(8)	0.25000(0)	0.21880(4)	6(1)
Er3	0.48680(8)	0.75000(0)	0.39860(5)	8(1)
Er4	0.18900(7)	0.75000(0)	0.02060(4)	6(1)
Er5	0.54920(7)	0.75000(0)	0.11510(4)	6(1)
Er6	0.12450(7)	0.75000(0)	0.43000(4)	6(1)
S1	0.04810(39)	0.25000(0)	0.07620(24)	5(1)
S2	0.94740(41)	0.25000(0)	0.42440(24)	6(1)
S3	0.32050(41)	0.75000(0)	0.18290(26)	7(1)
S4	0.73210(40)	0.25000(0)	0.12690(25)	5(1)
S5	0.63700(42)	0.75000(0)	0.28240(25)	7(1)
S6	0.63310(40)	0.25000(0)	0.46850(25)	7(1)
S7	0.99250(39)	0.25000(0)	0.73230(23)	4(1)
S8	0.28920(41)	0.25000(0)	0.36880(25)	6(1)
S9	0.61530(38)	0.75000(0)	0.96650(24)	4(1)

Table 3
Thermal parameters as $\exp(-2\Pi^2 \cdot \Sigma(U_{ij} \cdot a_i^* \cdot h_i \cdot h_j)) \cdot 10^3$

Atom	U_{11}	U_{22}	U_{33}	U_{12}	U_{13}	U_{23}
Er1	8(1)	7(1)	7(1)	0(0)	0(1)	0(0)
Er2	8(1)	7(1)	5(1)	0(0)	1(1)	0(0)
Er3	7(1)	6(1)	11(1)	0(0)	3(1)	0(0)
Er4	5(1)	6(1)	6(1)	0(0)	0(1)	0(1)
Er5	5(1)	6(1)	7(1)	0(0)	1(1)	0(0)
Er6	6(1)	7(1)	6(1)	0(0)	1(1)	0(0)
S1	2(2)	7(2)	6(2)	0(0)	−2(1)	0(0)
S2	7(2)	8(2)	3(2)	0(0)	0(1)	0(0)
S3	5(2)	5(2)	12(2)	0(0)	4(1)	0(0)
S4	3(2)	5(2)	6(2)	0(0)	0(1)	0(0)
S5	8(2)	8(2)	7(2)	0(0)	4(1)	0(0)
S6	5(2)	9(2)	6(2)	0(0)	0(1)	0(0)
S7	4(2)	5(2)	5(2)	0(0)	3(1)	0(0)
S8	6(2)	6(2)	5(2)	0(0)	0(1)	0(0)
S9	1(1)	5(2)	6(2)	0(0)	0(1)	0(0)

ε-Ln_2S_3, i.e. the α-Al_2O_3, structure type. The lanthanide sesquisulphides can exhibit other allotropic forms (see Ref. [11], where six polymorphs are reported for Yb_2S_3).

The high-temperature chemistry of the rare-earth sulphides is characterised by refractory behaviour (i.e. high melting points and low volatility) and that makes it very difficult to grow single crystals [12]. A large number of methods to prepare rare-earth chalcogenides has been described by Guittard and Flahaut [13].

In this work we report the results of the crystal growth procedure, X-ray structure determination and microstructural study of erbium sesquisulphide, Er_2S_3.

2. Experimental

The binary sulphide Er_2S_3 was prepared as a microcrystalline powder by induction heating a graphite crucible with Er_2O_3 (4N) in a stream of Ar (95%)+H_2S (5%) at 1773 K for 3 h and then cooling to room temperature by switching off the furnace. The product was heated in a sealed evacuated silica tube ($\varnothing_i = 11$ mm, length 30 cm) with iodine (4 mg/cc) as transport agent at 1373 K for 24 days with a gradient temperature of 125° and slowly cooled to room temperature. Single crystals up to 1 cm long were grown (see the scanning electron micrograph shown in Fig. 1).

The experimental conditions for the single-crystal X-ray diffraction are given in Table 1.

Electron microscopy/diffraction studies were carried out by means of a CM200 FEG electron microscope fitted with a double tilt (±35°) stage. For high-resolution imaging a JEOL 4000EX microscope was used. Due to the needle-shaped crystals, to avoid preferential cleavage of the crystals it was necessary to embed a few single needles in an epoxy resin and to cut them by ultramicrotomy perpendicular to the fibre axis. The cuts were then mounted onto copper grids coated with holey carbon supported films.

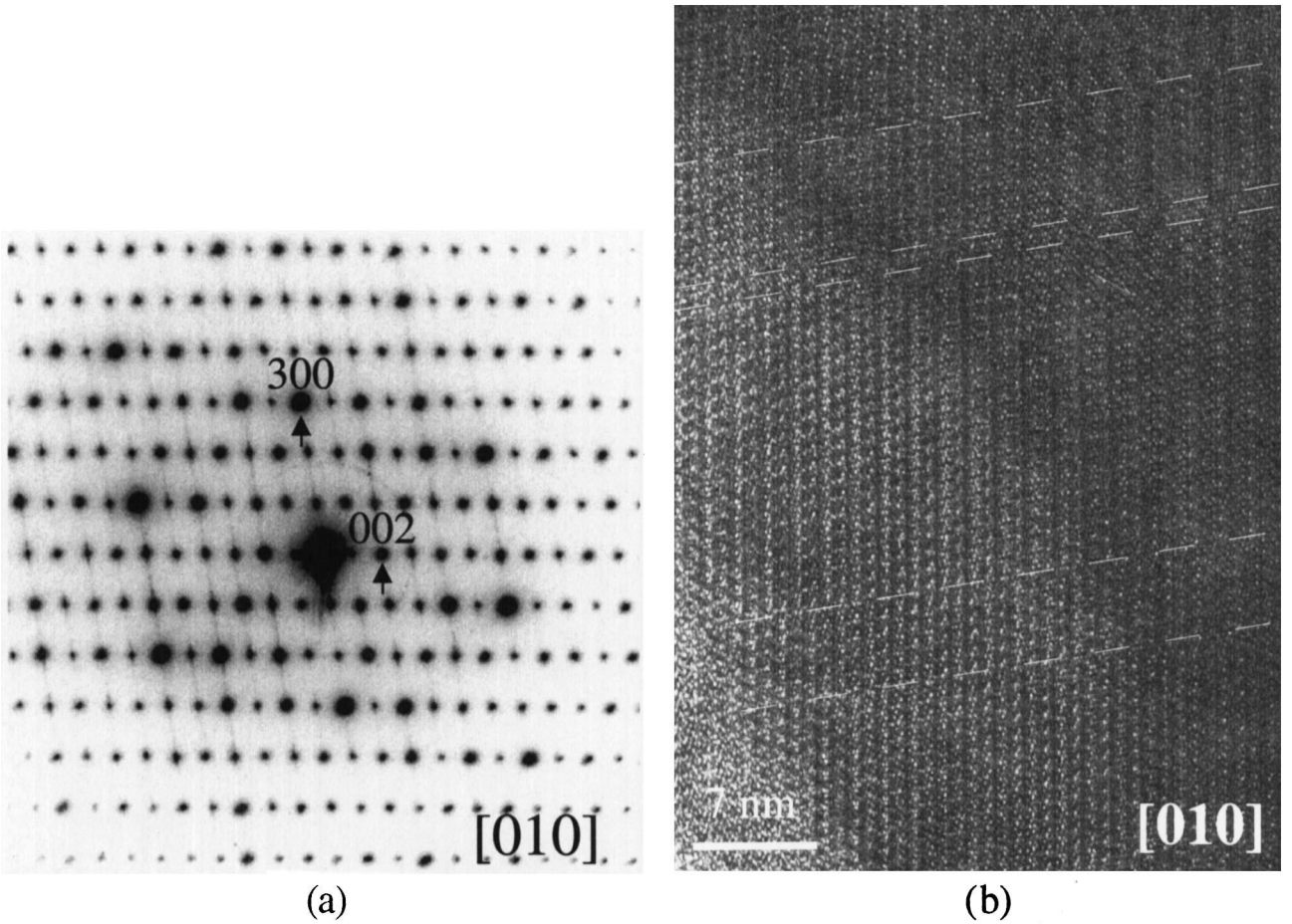

Fig. 4. (a) SAED pattern of a δ-Er_2S_3 crystal showing diffuse intensity streaking along the [100]* direction due to the presence of extended defects. (b) Electron micrograph of a δ-Er_2S_3 crystal which shows extended defects perpendicular to the [100] direction.

3. Results

3.1. X-ray structure determinations

In Fig. 1a the SEM micrograph shows the typical shape of Er_2S_3 crystals. One of these yellow coloured crystals with a well-defined needle-like shape was coated with epoxy resin and mounted in a kappa diffractometer. The cell dimensions were refined by least-squares fitting the θ values of 25 well centred reflections within a 2θ range of 13–35°.

The intensities were corrected for Lorentz and polarisation effects. Scattering factors for neutral atoms and anomalous dispersion corrections for Er and S were taken from the *International Tables for X-Ray Crystallography* [14].

The structure was solved by Patterson and Fourier methods. Interpretation of the Patterson function was achieved by the superposition method proposed by Clastre and Gay [15] and is discussed in detail in Ref. [16]. The sulphur atoms were located by Fourier synthesis.

An empirical absorption correction [17] was applied at the end of the isotropic refinements. A final refinement was undertaken with unit weights and anisotropic thermal motion.

No trend in ΔF vs. F_o or $\sin\theta/\lambda$ was observed. Final difference synthesis showed no significant electron density.

The atomic refined parameters are shown in Tables 2 and 3. The structure is isostructural with δ-Ho_2S_3 with Er atoms in coordination 6 and 7. A schematic drawing of the structure is shown in Fig. 2.

3.2. Transmission electron microscopy

Fig. 3 shows a selected area electron diffraction pattern (SAED) along the short axis, i.e. along the [010] zone axis, showing well-defined maxima due to the δ-Er_2S_3 structure plus diffuse maxima, the origin of which is discussed below. Although the majority of the crystals did not show the presence of extended defects, in a very few exceptional cases extended defects were observed perpendicular to the [100] direction (see the SAED pattern of Fig. 4a). Unfortunately, the defects could only be observed in the thick part of the crystal and no conclusive information about its nature can be extracted from the high-resolution image. However, from the contrast observed in the micrograph (see Fig. 4b), it can be considered that the disorder is possibly due to the presence of antiphase boundaries.

High-resolution images of the crystal usually show high order. When the images are obtained close to the Scherzer focus (see Fig. 5a), the contrast is dominated by the Er atoms. Simulation of the high-resolution image along the [010] direction confirms that the dark spots observed in the experimental image correspond to the positions of the Er atoms. The best fitting was found for a thickness of 12 nm and a defocus of 60 nm. The simulated image is inset as Fig. 5b.

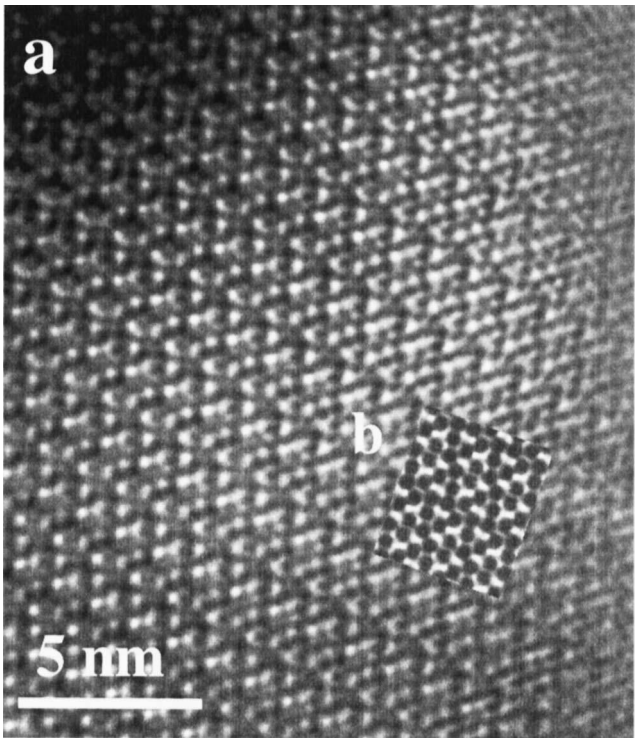

Fig. 5. (a) High-resolution electron micrograph of a δ-Er_2S_3 crystal orientated along the [010] direction. (b) Simulation of the HREM image calculated from the atomic coordinates refined by single-crystal X-ray diffraction. The image was calculated for a thickness of 12 nm and a defocus of 60 nm.

During observation of the Er_2S_3 crystals by HREM they were shown to be electron radiation sensitive and the edges of the crystal are damaged very quickly. This damage did not produce an amorphous edge directly, but formed crystallites with an apparently simpler structure than Er_2S_3. Fig. 6a shows an enlargement of the edge of the crystal shown in Fig. 5. The power spectrum obtained by computer fast Fourier transform of the image is shown in Fig. 6b. Notice the extra blurred diffraction maxima which correspond to the crystallites formed on the edge. These blurred diffraction maxima could be indexed in the [110] zone axis of a fcc unit cell. Using the δ-Er_2S_3 diffraction maxima of the power spectrum as internal standard the calculated a parameter for the fcc unit cell is 5.3 Å, which fits with the unit cell parameter of ErS with a cubic fcc unit cell and $a \approx 5.430$ Å [18]. Consequently, the electron beam damage of δ-Er_2S_3 consists of the reduction of the erbium atoms by the electron beam to generate the higher symmetry NaCl-type structure of ErS. In addition, either a loss of sulphur and/or the formation of a large quantity of vacancies has to be considered.

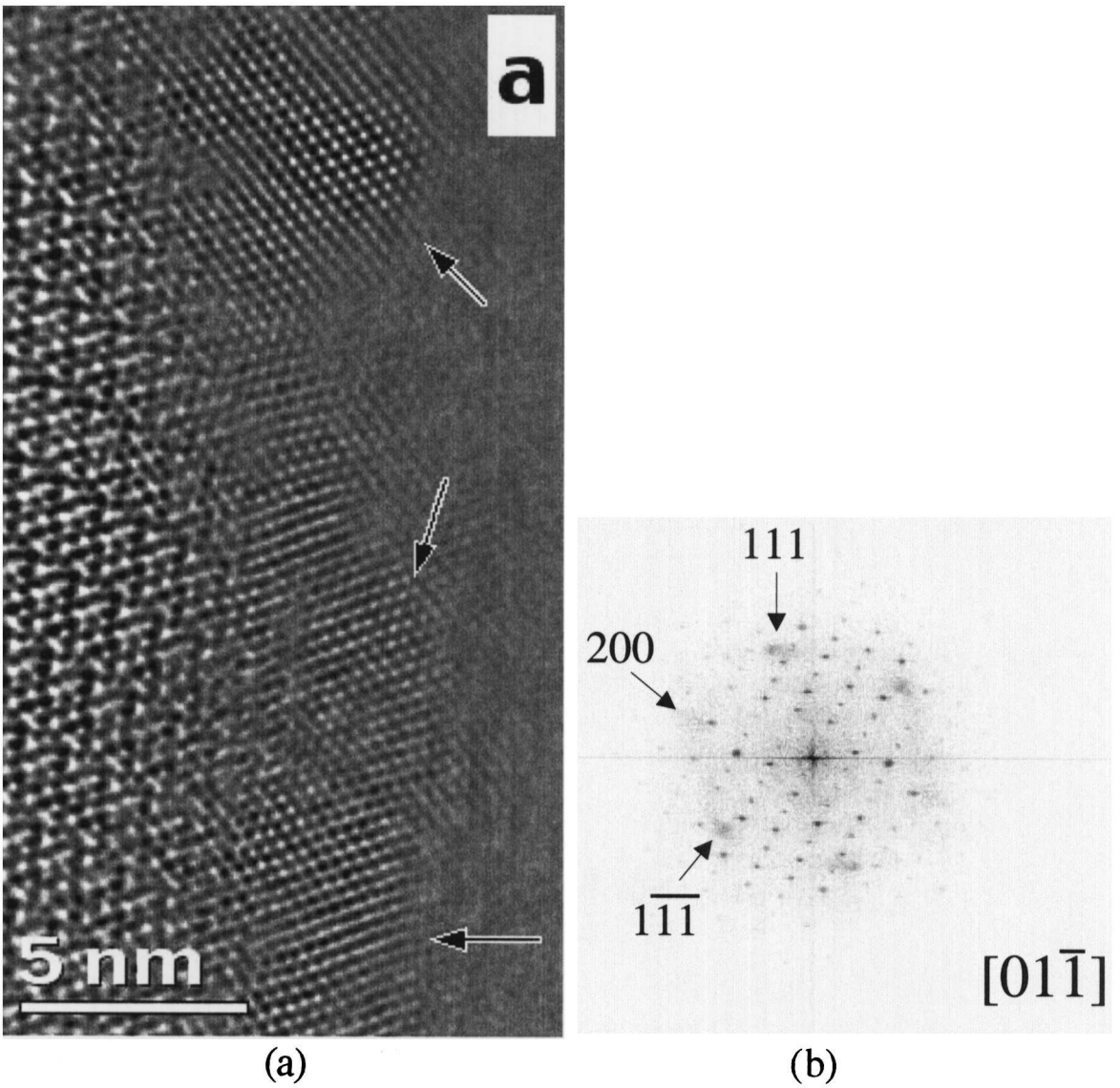

Fig. 6. (a) HREM image of the crystallites formed on the edge of the crystal due to electron beam damage. (b) Power spectrum obtained by computer fast Fourier transform of the image shown in (a).

Acknowledgements

This work was supported by CYCIT project MAT-0697.

References

[1] J. Flahaut, in: K.A. Gschneidner, L. Eyring (Eds.), Handbook on the Physics and Chemistry of Rare Earths, Vol. 4, 1979, p. 1, and references cited therein.
[2] H.F. Franzen, R.T. Tuenge, L. Eyring, J. Solid State Chem. 49 (1983) 206.
[3] L.C. Otero-Díaz, A.R. Landa-Cánovas, B.G. Hyde, J. Solid State Chem. 89 (1990) 237.
[4] L.C. Otero-Díaz, in: R. Sáez, P. Caro (Eds.), Rare Earths, Complutense S.A, 1998, p. 67.
[5] A.W. Sleight, C.T. Prewit, Inorg. Chem. 7 (1968) 2282.
[6] B.G. Hyde, S. Andersson, Inorganic Crystal Structures, Wiley, 1989.
[7] D. Carre, P. Laruelle, P. Besançon, C.R. Acad. Sci. Paris C 270 (1970) 537.
[8] W.H. Zacariasen, Acta Crystallogr. 2 (1949) 57.
[9] J.M. Tourre, Safer red pigments for plastics, Rare Earth Information Center News, Sept. 1, No. 3, 1993.
[10] S. Romero, A. Mosset, P. Macaudiere, J.C. Trombe, J. Alloys Comp. 302 (2000) 118.
[11] A.A. Eliseev, G.M. Kuz'micheva, V.I. Yashnov, J. Inorg. Chem. 23 (2) (1978) 273.
[12] A.V. Prokofiev, A.I. Shelykh, A.V. Golubkov, I.A. Smirnov, J. Alloys Comp. 219 (1995) 172.

[13] M. Guittard, J. Flahaut, in: G. Meyer, L.R. Morss (Eds.), Synthesis of Lanthanide and Actinide Compounds, Kluwer Academic, 1991, p. 321.
[14] International Tables for X-Ray Crystallography, Vol. IV, Kynoch Press, Birmingham, UK, 1974, p. 72.
[15] J. Clastre, R. Gay, Compt. Rend. 320 (1950) 1876.
[16] U. Shmueli (Ed.), International Tables for Crystallography, Vol. B, Kluwer Academic, Dordrecht, 1993, p. 230.
[17] N. Walker, D. Stuart, Acta Crystallogr. A39 (1983) 158.
[18] J. Flahaut, P. Laruelle, in: L. Eyring (Ed.), Progress in the Science and Technology of the Rare Earths, Vol. III, Pergamon Press, 1968, p. 149.